Biosensors and Bioelectronics 50 (2013) 437–440

Contents lists available at SciVerse ScienceDirect

Biosensors and Bioelectronics

journal homepage: www.elsevier.com/locate/bios

Label free redox capacitive biosensing

Flávio C. Bedatty Fernandes [a], Márcio S. Góes [a], Jason J. Davis [b,1], Paulo R. Bueno [a,*]

[a] Instituto de Química, Universidade Estadual Paulista, CP 355, 14800-900 Araraquara, São Paulo, Brazil
[b] Department of Chemistry, University of Oxford, South Parks Road, Oxford OX1 3QZ, UK

ARTICLE INFO

Article history:
Received 15 May 2013
Received in revised form
19 June 2013
Accepted 20 June 2013
Available online 2 July 2013

Keywords:
Capacitance spectroscopy
Immunosensors
Biosensor
Redox capacitance

ABSTRACT

A surface confined redox group contributes to an interfacial charging (quantifiable by redox capacitance) that can be sensitively probed by impedance derived capacitance spectroscopy. In generating mixed molecular films comprising such redox groups, together with specific recognition elements (here antibodies), this charging signal is able to sensitively transduce the recognition and binding of specific analytes. This novel transduction method, exemplified here with C-reactive protein, an important biomarker of cardiac status and general trauma, is equally applicable to any suitably prepared interfacial combination of redox reporter and receptor. The assays are label free, ultrasensitive, highly specific and accompanied by a good linear range.

© 2013 Elsevier B.V. All rights reserved.

1. Introduction

The electrochemical interrogation of biorecognition at man-made interfaces constitutes a potentially powerful means of establishing highly effective, cheap and portable diagnostic assays (Berggren et al., 2001; Davis and Tkac, 2009; Estrela et al., 2010; White et al., 2012; Xu et al., 2013; Eckermann et al., 2010; Bueno and Gabrielli, 2008). Within these, impedimetric tools, based on Electrochemical Impedance Spectroscopy (EIS), constitute potent, label free, and ultrasensitive probes of antibody–antigen or peptide–protein interactions on suitably modified electrode surfaces (Lisdat and Schäfer, 2008; Bryan et al., 2013; Johnson et al., 2012; Daniels and Pourmand, 2007; K'Owino and Sadik, 2005; Bryan et al., 2012). In its simplest and most common modality, the formation of bioaffinity complexes retards the interfacial electron transfer kinetics associated with a solution phase redox probe. The quantification of this "charge transfer resistance" (R_{ct}) is, then, the transducing signal used to quantify target analyte concentration across, typically, nanomolar to picomolar concentration limits (Lisdat and Schäfer, 2008; Daniels and Pourmand, 2007; Rodriguez et al., 2005; Bogomolova et al., 2009). In recent years there has been progress in moving such assays to the analysis of real clinical samples (Bryan et al., 2013; Johnson et al., 2012; Bryan et al., 2012).

The use of R_{ct} does, however, require the application of a redox probe to the analytical solution prior to analysis, and a subsequent fitting of data to an "equivalent circuit". In recent work we have introduced a detailed capacitance analysis of pure dielectric and redox active molecular films and, in particular, electroactive monolayer capacitance spectroscopy, EMCS (Bueno et al., 2012a, 2012b; Goes et al., 2012).

We show herein that the redox capacitance of a faradaic probe *confined* within a molecular film is a sensitive function of protein biomarker concentration when that film is additionally capable of selectively recruiting the target from solution.

In principle, a number of electrochemical techniques might be utilised, in each case resulting in interrogating the probe output as a function of its local environment and any deliberately engineered local binding events (White et al., 2012; Elliott et al., 1986; Liu et al., 2008; Sumner and Creager, 2001). For example, voltammetric methods have been proposed where the current response to an applied voltage is reported to detect antigen binding when the probe is tethered to the antibody or aptamer receptor (Johnson et al., 2012; Rodriguez et al., 2005; Darwish et al., 2012a, 2012b; Gooding and Darwish, 2012; Liu et al., 2008). Although analytically simple, these assays require the pre-synthesis of a receptor–redox conjugate and, in the case of aptamers, a predictable target induced conformational change (a change very often highly dependent on solution composition) (Rodriguez et al., 2005; Liu et al., 2008; Darwish et al., 2012a, 2012b; Gooding and Darwish, 2012; Liu et al., 2008).

We have recently shown that the EIS derived complex capacitance signal can be used to generate an interfacial charging signal that arises solely from the redox activity of a confined group (its redox capacitance, C_r) and depends very sensitively of its electrostatic environment. We start here by noting that C_r of a surface confined electroactive film is not a common electrostatic capacitance

* Corresponding author. Tel.: +55 16 3301 9642; fax: +55 16 3322 2308.
E-mail addresses: jason.davis@chem.ox.ac.uk (J.J. Davis), prbueno@iq.unesp.br (P.R. Bueno).
[1] Tel.: +44 1865 275914.

0956-5663/$ - see front matter © 2013 Elsevier B.V. All rights reserved.
http://dx.doi.org/10.1016/j.bios.2013.06.043

whose potential depends exclusively on dimensions. It is, rather, a capacitance whose occupation/magnitude depends on redox centre energy levels and occupancy (Bueno et al., 2012a). The population of these states, of course, dictates commonly observed associated cyclic voltammetric (CV) peaks and depends on Fermi–Dirac statistics in a way that non faradaic contributions (Bueno et al., 2012a, 2012b) to current, such as those involved in ionic relaxation, do not. Faradaic current, directly reporting C_r occupancy, specifically depends on electrode potential according to $f = n/\Gamma = F(E_r, \mu_e)$, were μ_e is the electron chemical potential (or the Fermi level, E_F) and n is the number of occupied redox centres. In considering a single redox energy state, E_r, C_r is directly proportional to the redox molecular surface coverage, Γ, according to (Bueno et al., 2012a, 2012b)

$$C_r = e^2\Gamma\frac{df}{d\mu_e} = \frac{e^2\Gamma}{k_BT}f(1-f) \quad (1)$$

and the faradaic current is $j_f = C_r s$, where s is the voltage scan rate (Bueno et al., 2012b). In Eq. (1) e is the elementary charge, k_B the Boltzmann constant and T the absolute temperature. Note that [Eq. (1)] both C_r and cyclic voltammetry resolved peak current are maximised, when $f = 1/2$ and $f(1-f) = 1/4$, i.e. at the half-wave potential (Bueno et al., 2012a, 2012b). We show herein that this C_r signal sensitively and selectively transduces the interfacial binding of specific targets at suitably prepared interfaces.

2. Experimental procedure

2.1. Experimental Procedures and Methods

Gold electrodes disks (2.0 mm diameter, Metrohm) were mechanically polished with decreasing particle size aluminium oxide pads (1 μm, 0.3 μm and 0.05 μm) with sonication in water (18.2 MOhm, Millipore). Electrodes were then electrochemically polished in deaerated NaOH 0.5 M (−1.5 V and −0.5 V at a scan rate of 100 mV s^{-1}) and 0.5 M H_2SO_4 (−0.2 V and 1.5 V at a scan rate of 100 mV s^{-1}) until the gold reduction peak in CV stabilizes (around 50 cycles). After electrochemical polishing the electroactive areas were evaluated by integration of the cathodic peak from gold electropolishing voltammograms and converted to the real surface area using a conversion factor of 400 μC cm^{-2} (Trasatti and Petrii, 1991). Finally, the polished gold electrode was characterized by Cyclic Voltammetry (CV) and Capacitance Spectroscopy (CS).

Electrochemical measurements were performed with an Autolab potentiostat model PGSTAT30 using a three-electrode configuration with Ag/AgCl (3 M in KCl) as a reference, platinum mesh as a counter, and functionalized gold electrode as the working electrode.

Mixed Self-Assembled Monolayers (SAM) were generated by incubation of freshly cleaned gold electrodes in a solution of 0.2 mM pentadecanethiol and 2.0 mM 11-ferrocenyl-undecanethiol in ethanol for 16 h, prior to washing in alcohol, deionized water and drying under nitrogen. Receptive surfaces were prepared by immersion of these in 1 μM anti-CRP in 0.1 M bicarbonate buffer, pH 8.5 prior to analysis by Capacitance Spectroscopy and CV. C-Reactive Protein (CRP) aliquots (20 μl) were added to the interface with concentrations ranging from 0.5 nM to 10.0 nM in PBS (pH 7.4). The current density (or its variation as a function of CRP binding) in CV measurements (Fig. 2) is directly derived from that measured at half-wave potential. C_r (or its reciprocal) is resolved at the same potential at a frequency (here optimized at 8 Hz, i.e. a value close to the time scale of faradaic electron transfer).

2.2. Capacitance spectroscopy

The AC frequencies for impedance experiments ranged from 1 MHz to 10 mHz, with an amplitude of 10 mV. All the obtained impedance data were checked regarding to compliance with the constraints of linear systems theory by Kramers–Kronig using the appropriate routine of the FRA AUTOLAB software. Impedance data were acquired at half wave potential (*redox in*) and non fardaic (*redox out)* regions (see main text and Fig. 2 therein). Modulation frequencies were varied in 80 steps from 0.1 mHz to 10 MHz.

The complex $Z^*(\omega)$ (impedance) function was converted into $C^*(\omega)$ (capacitance) through the physical definition $Z^*(\omega) = 1/j\omega C^*(\omega)$ in which ω is the angular frequency. A previously outlined EMCS analysis was then performed (Bueno et al., 2012a) to resolve potential regions of maximum and minimum faradaic activity, i.e. previously noted “redox in” and “out” regions. The resulting FRA data were processed and treated to obtain the imaginary part of the capacitance as mentioned previously, i.e. $Z^* = 1/j\omega C^*$. From this operation, note that $C'' = \varphi Z'$ and $C' = \varphi Z''$, where $\varphi = (\omega|Z|^2)^{-1}$ and $|Z|$ is the modulus of Z^*. The advantages associated with using the outlined EMCS approach is that the end user eliminates the capacitive and resistive “parasitic” terms related to the non-electroactive components inherent in any given film (Bueno et al., 2012a, 2012b).

2.3. Negative controls and non-receptive films

Negative controls were carried out by both dosing mixed 11-ferrocenyl-undecanethiol and pentadecanethiol (9:1) films tested with equivalent concentrations of BSA (the negative control) and, separately, in examining the response of pure 11-ferrocenyl-undecanethiol films, without anti-CRP antibody, to CRP.

3. Results and discussion

The thermodynamic and kinetic fingerprint associated with surface confined redox active groups is known to be a sensitive function of solvation and counter ion/electrolyte access (Bryan et al., 2012; Elliott et al., 1986; Liu et al., 2008; Sumner and Creager, 2001). Our hypothesis was that this fingerprint, nicely resolved by impedance spectroscopy derived capacitance methods, could sensitively report on the binding of biological targets at local surface sites through associated change in local dielectric and electrolyte access. As an initial proof of concept, we develop and utilise herein a redox active interface capable of the selective recruitment of CRP (C-Reactive protein), an acute phase protein whose levels in blood are indicative of cardiac status and general inflammation (Bryan et al., 2013; Johnson et al., 2012; Gabay and Kushner, 1999). Molecular films comprising a mixed layer of pentadecanethiol associated with anti-CRP antibody diluted within a 11-ferrocenyl-undecanethiol (1:9) film (Fig. 1) were, specifically used to report on target CRP binding. As shown in Fig. 2, a simple CV resolved film response is an adequate function of CRP concentration but, notably, this is not sufficiently so or indeed selective (being both frequency unresolved and a composite summation of redox, resistance and charging contributions) at these interfaces for its reporting to be analytical useful (Bueno et al., 2012a, 2012b).

In summary, the initial on-film assembly of the antibody is associated with both an anodic shift and drop in response of the prepared mixed film to levels which, in the absence of CRP, are thereafter stable. Subsequent CRP binding results in a progressive change in response. As shown in Fig. 2*b*, these changes are, though, not analytically useful. The target induced perturbation in film faradaic activity is more sensitively probed by capacitance,

where the resolved signal is able to track target binding much more sensitively than possible by traditional EIS resolved impedance (Fig. 3).

To be clear, this analytical methodology is distinct from that offered by traditional impedance, where interfacial Z'' or charge transfer resistance is reported (the latter after data fitting) (Johnson et al., 2012). The resolved insensitivity, at any surface potential poise, of Z' to the binding of a specific target (Fig. 3*a*) arises directly because the transducing signal measured is not based on charge transfer resistance but faradaic capacitive charging. Thus, in converting the same raw data into complex capacitance an analogous Nyquist diagram (Fig. 3*b*) shows clearly that interfacial recognition can be sensitively detected. As shown in Fig. 4, both the real and imaginary capacitive components are highly responsive. In acquiring such data initially at a non fararadaic surface potential poise and then again at the ferrocene probe half wave potential, the purely faradaic capacitive term, C_r, is resolved (Bueno et al., 2012a). In doing this it is also evident that capacitive contributions outside of the redox window are small and unresponsive. As shown in Fig. 5, C_r is itself a highly sensitive analytical function.

The same figure also illustrates the selectivity of this interfacial charging response to CRP the average response of these interfaces to a nonspecific negative control protein is less than 8% over the same concentration range. The nonreceptive Fc control films do not respond to CRP or BSA across an equivalent range of concentrations.

From these analyses, the limit of detection (L.O.D), limit of quantification (L.O.Q) and percentage sensitivity per decade were, respectively, 200 pM, 600 pM and 95% according to IUPAC standardization (Long and Winefordner, 1983), comparing favourably to previous assays of this target (Bryan et al., 2013; Johnson et al., 2012; Bryan et al., 2012).

4. Conclusions

In summary, we have demonstrated herein, a novel and label free means of detecting specific protein targets at suitably modified electrodes with good reproducibility and sensitivity. This capability is fully based on the capacitive response of a redox modified electrode and the sensitivity of this to local dielectric and

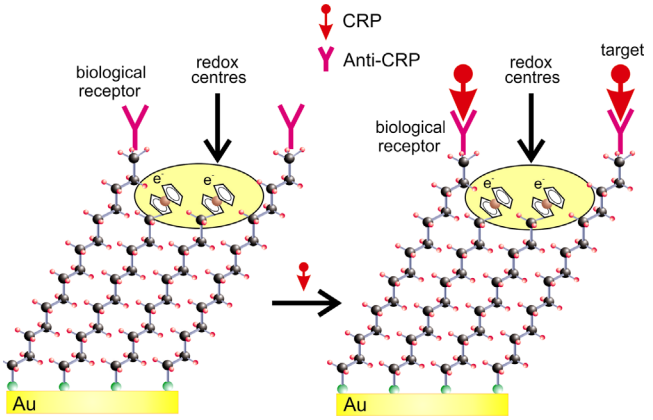

Fig. 1. Schematic representation (not to relative scale) of an electroactive and target receptive molecular film comprising a mixed monolayer of antiCRP antibody and alkyl ferrocene redox probe (prepared from a 9:1 M mix of 11-ferrocenyl-undecanethiol and pentadecanethiol). The antiCRP moieties are assembled on the alkanethiol layer by means of stable hydrophobic association. The electroactive centres transduce the CRP target binding event into a modulated electronic signal through redox capacitance.

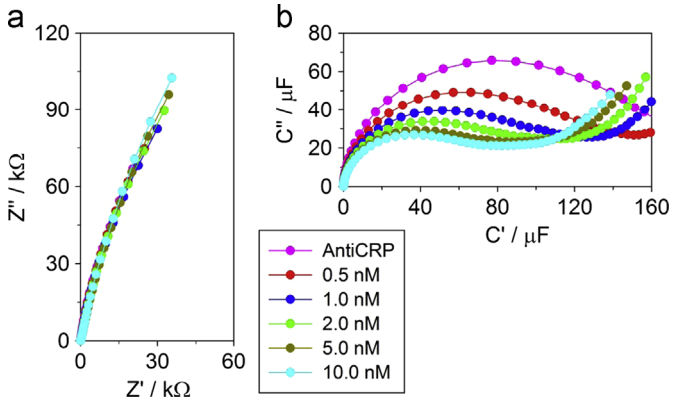

Fig. 3. Faradaic impedance analyses resolve the unresponsiveness and sensitivity of interfacial impedance and capacitance respectively. (a) Nyquist impedimetric plot of Z'' versus Z' for a redox active, CRP-receptive film, where only minimal sensitivity to target binding is evident. The analogous capacitative response to CRP binding is shown in (b) where a sensitive modulation in response to CRP is observed (C_r itself is obtained from the semicircle diameters). All plots are average curves obtained from three different working electrodes.

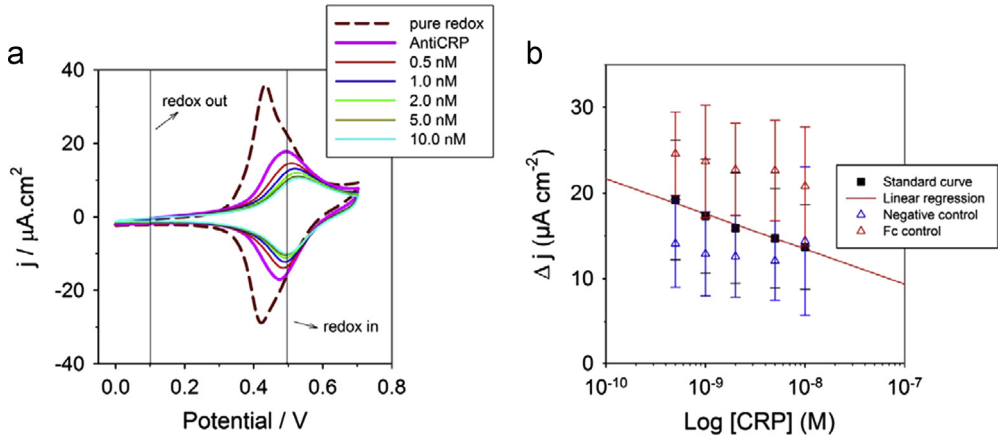

Fig. 2. (a) CV resolved perturbations in faradaic activity of a redox active, CRP-recruiting molecular film (see Fig. 1) in the presence of different target concentrations at a scan rate of 100 mV s^{-1}. All plotted curves are mean values of three different working electrodes. The *redox in* and *out* lines denote potential regions where EMCS was performed, as detailed in the text. (b) Comparative CV derived response in current density to CRP target where the relative insensitivity and marked nonspecific nature of the perturbation is clear (the negative controls and Fc control data sets respond in a comparable way to the current density of an intentionally CRP binding interface). This (CV) derived approach is clearly not viable from an assay perspective (the signal perturbation being neither specific nor large). The error bars indicate variance across triplicate measurements (3 independent assaying surfaces).

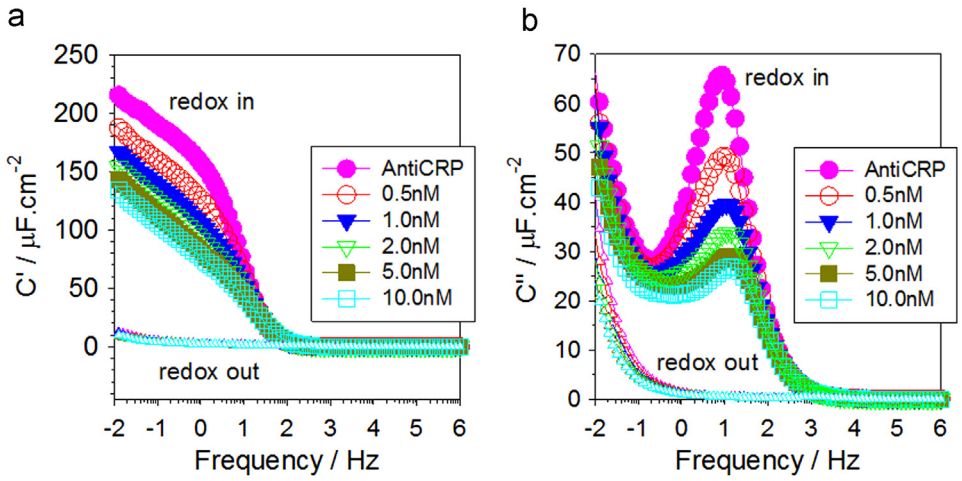

Fig. 4. (a) The real part of the molecular film complex capacitance at electrode potentials corresponding to (*redox in*) or removed from (*redox out*) the ferrocene reporter half wave potential. (b) The same as (a) but showing the imaginary part of complex capacitance response. Note that frequency axis is reported here as base ten exponents. All plots are average curves obtained from three different immunoassay working electrodes (prepared from a 9:1 molar mix of 11-ferrocenyl-undecanethiol and pentadecanethiol) initially modified with anti-CRP (purple) then incubated in progressively higher target concentrations. (For interpretation of the references to color in this figure legend, the reader is referred to the web version of this article).

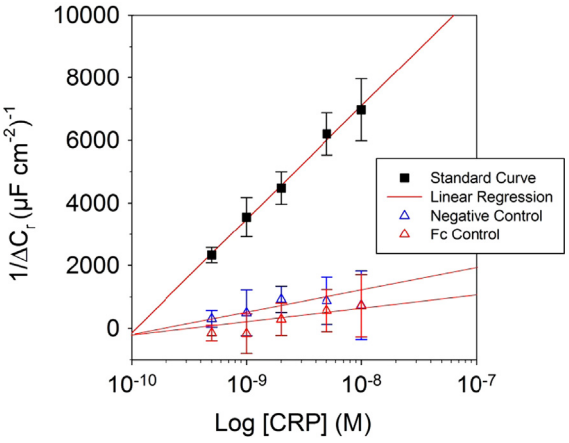

Fig. 5. Capacitive analytical curves acquired at 8 Hz with receptive and redox active molecular films. Also shown are both the unresponsiveness of mixed film charging in the absence of CRP (the negative control) and the unresponsiveness of a pure alkanethiol layer to different CRP target concentration (Fc control). The Pearson linear coefficient is higher than 99%. The error bars indicate variance across triplicate measurements (3 independent assaying surfaces).

local redox states. Applied here in establishing a potent assay of CRP, it is notable that interfacial impedance is insensitive to this target under the same conditions (confirming transduction to be capacitive). In contrast to traditional impedance methods, no redox element is added to solution and no equivalent circuit necessarily considered or fitted to. The methodology is experimentally simple, frequency optimized, and likely to be equally applicable to a broad range of target:receptor combinations.

Acknowledgements

This work was supported by the São Paulo state research funding agency (FAPESP) and São Paulo State University (UNESP) grants. Flávio Bedatty acknowledges the CNPq (Brazilian National Research Council) for his PhD scholarship and grants.

References

Berggren, C., Bjarnason, B., Johansson, G., 2001. Electroanalytical 13 (3), 173–180.
Bogomolova, A., Komarova, E., Reber, K., Gerasimov, T., Yavuz, O., Bhatt, S., Aldissi, M., 2009. Analytical Chemistry 81, 3944–3949.
Bryan, T., Luo, X., Forsgren, L., Morozova-Roche, L.A., Davis, J.J., 2012. Chemical Science 3 (12), 3468–3473.
Bryan, T., Luo, X., Bueno, P.R., Davis, J.J., 2013. Biosensors Bioelectronics 39 (1), 94–98.
Bueno, P.R., Gabrielli, C., 2008. Electrochemistry, Nanomaterials and Nanostructures. In: L, E.R. (Ed.), Handbook of Nanostructured Materials for Alternative Energy Device. Springer, New York. (Org.).
Bueno, P.R., Davis, J.J., Mizzon, G., 2012a. Journal of Physical Chemistry C 116 (30), 8822–8829.
Bueno, P.R., Fabregat-Santiago, F., Davis, J.J., 2012b. Analyical Chemistry 85, 411–417.
Daniels, J.S., Pourmand, N., 2007. Electroanalysis 19 (12), 1239–1257.
Darwish, N., Diez-Perez, I., Guo, S., Tao, N., Gooding, J.J., Paddon-Row, M.N., 2012a. Journal of Physical Chemistry C 116 (39), 21093–21097.
Darwish, N., Eggers, P.K., Ciampi, S., Tong, Y., Ye, S., Paddon-Row, M.N., Gooding, J.J., 2012b. Journal of the American Chemical Society 134 (44), 18401–18409.
Davis, J.J., Tkac, J., 2009. Label free field effect protein detection. In: Davis, J.J. (Ed.), Engineering the Bioelectronic Interface. The Royal Society of Chemistry, London.
Eckermann, A.L., Feld, D.J., Shaw, J.A., Meade, T.J., 2010. Coordination Chemistry Reviews 254, 1769–1802.
Elliott, C.M., Redepenning, J.G., Balk, E.M., 1986. Journal of Electroanalitical Chemistry 213 (2), 203–215.
Estrela, P., Paul, D., Song, Q., Stadler, L.K.J., Wang, L., Huq, E., Davis, J.J., Ferrigno, P.K., Migliorato, P., 2010. Analytical Chemistry 82 (9), 3531–3536.
Gabay, C., Kushner, I., 1999. New England Journal of Medicine 340 (6), 448–454.
Goes, M.S., Rahman, H., Ryall, J., Davis, J.J., Bueno, P.R., 2012. Langmuir 28 (25), 9689–9699.
Gooding, J.J., Darwish, N., 2012. Chemical Records 12 (1), 92–105.
Johnson, A., Song, Q., Ferrigno, P.K., Bueno, P.R., Davis, J.J., 2012. Analytical Chemistry 84 (15), 6553–6560.
K'Owino, I.O., Sadik, O.A., 2005. Electroanalysis 17 (23), 2101–2113.
Lisdat, F., Schäfer, D., 2008. Analytical and Bioanalytical Chemistry 391 (5), 1555–1567.
Liu, G., Paddon-Row, M.N., Gooding, J.J., 2008. Chemical Communications 33, 3870–3872.
Liu, G., Paddon-Row, M.N., Gooding, J.J., 2008. Chemical Communications 33, 3870–3872.
Long, G.L., Winefordner, J.D., 1983. Analytical Chemistry 55 (7), 712–724.
Rodriguez, M.C., Kawde, A.-N., Wang, J., 2005. Chemical Communication 34, 4267–4269.
Sumner, J.J., Creager, S.E., 2001. Journal of Physical Chemistry B 105 (37), 8739–8745.
Trasatti, S., Petrii, O.A., 1991. Pure and Applied Chemistry Chimie pure et appliquée 63, 711–734.
White, R.J., Kallewaard, H.M., Hsieh, W., Patterson, A.S., Kasehagen, J.B., Cash, K.J., Uzawa, T., Soh, H.T., Plaxco, K.W., 2012. Analytical Chemistry 84 (2), 1098–1103.
Xu, M.Y., Luo, X.L., Davis, J.J., 2013. Biosensors and Bioelectronics 39 (1), 21–25.